

Maximum-Likelihood Detection in DWT Domain Image Watermarking Using Laplacian Modeling

T. M. Ng, *Student Member, IEEE*, and H. K. Garg

Abstract—Digital image watermarks can be detected in the transform domain using maximum-likelihood detection, whereby the decision threshold is obtained using the Neyman–Pearson criterion. A probability distribution function is required to correctly model the statistical behavior of the transform coefficients. Earlier work has considered modeling the discrete wavelet transform coefficients using a Gaussian distribution. Here, we introduce a Laplacian model and establish via simulation that it can result in a better performance than the Gaussian model.

Index Terms—Discrete wavelet transform, Laplacian, maximum-likelihood (ML) detection, Neyman–Pearson.

I. INTRODUCTION

MAXIMUM-LIKELIHOOD (ML) detection schemes based on Bayes' decision theory have been considered for image watermarking in transform domain [1], [5], [6]. The Neyman–Pearson criterion is used to derive a decision threshold to minimize the probability of missed detection, subject to a given probability of false alarm. To achieve optimum behavior of the ML detector, a probability distribution function (PDF) that correctly models the distribution of the transform coefficients is required. In [1], magnitudes of the discrete Fourier transform (DFT) coefficients are modeled using a Weibull PDF. The discrete wavelet transform (DWT) coefficients are modeled using a Gaussian PDF in [5] and zero mean generalized Gaussian PDF in [6].

In this letter, we consider the ML detection scheme by modeling the DWT coefficients using a Laplacian PDF. We note that the zero mean generalized Gaussian model in [6] requires estimation of the shape parameter using function interpolation. In this regard, the Laplacian and Gaussian models are considered simpler models, and our focus here is on comparing watermark robustness under these two models in the DWT domain.

The letter is organized as follows. The embedding rule used with ML detection is given in Section II. The decision rule and threshold of ML detection are briefly explained in Sections III and IV, respectively. A more detailed description can be found in [1] and [6]. Section V shows the modeling of the DWT coefficients by a Laplacian PDF. Experimental results are shown in Section VI. The work is concluded in Section VII.

Manuscript received June 22, 2004; revised October 5, 2004. This work was supported by a research grant from the National University of Singapore. The associate editor coordinating the review of this manuscript and approving it for publication was Dr. Petr Tichavsky.

The authors are with the Department of Electrical and Computer Engineering, Faculty of Engineering, National University of Singapore, Singapore 117576, Singapore (e-mail: elengt@m@nus.edu.sg).

Digital Object Identifier 10.1109/LSP.2005.843776

The notation used is as follows. Nonbold letters are used to represent scalar quantities, sets, and functions. Bold letters are used for vectors. All vectors are real valued and expressed in column form.

II. WATERMARK INSERTION

Let $\mathbf{x} = [x_1 \ x_2 \ \cdots \ x_N]^T$ and $\mathbf{y} = [y_1 \ y_2 \ \cdots \ y_N]^T$ be N -vectors representing transform coefficients of an original image and the associated watermarked image, respectively. A watermark $\mathbf{w} = [w_1 \ w_2 \ \cdots \ w_N]^T$, which is chosen from a set M , is embedded into \mathbf{x} , giving \mathbf{y} . The elements x_i, w_i and y_i are viewed as realizations of the random variables X_i, W_i and Y_i , the underlying PDFs being $f_{X_i}(x_i), f_{W_i}(w_i)$ and $f_{Y_i}(y_i)$, respectively, for $i = 1, 2, \dots, N$. In ML detection scheme, \mathbf{w} is usually embedded into \mathbf{x} using the multiplicative rule, which is defined as

$$y_i = x_i(1 + \alpha_i w_i), \quad i = 1, 2, \dots, N \quad (1)$$

where α_i is a positive scalar representing the embedding strength. The embedding strength is tuned to provide a tradeoff between robustness and imperceptibility of the watermark.

III. ML DETECTION

The elements of the watermarks from the set M are assumed to be independent and uniformly distributed in the interval $[-1, 1]$. Specifically, if $\mathbf{w}^* = [w_1^* \ w_2^* \ \cdots \ w_N^*]^T$ is the embedded watermark, we can write $M = M_0 \cup M_1$, where $M_0 = \{\mathbf{w} : \mathbf{w} \neq \mathbf{w}^*\}$ and $M_1 = \{\mathbf{w}^*\}$. Note that the null watermark $\mathbf{w} = \mathbf{0} = [0 \ 0 \ \cdots \ 0]^T$ is already included in M_0 .

The decision rule in ML detection is as follows. The watermark \mathbf{w}^* is detected if the likelihood ratio $l(\mathbf{y}) = f_{\mathbf{Y}}(\mathbf{y} | M_1) / f_{\mathbf{Y}}(\mathbf{y} | M_0) > \lambda$, where $f_{\mathbf{Y}}(\mathbf{y} | M_j), j = 0, 1$ are the conditional PDFs, and λ is the decision threshold. For the watermark to be imperceptible, the embedding strength α_i is set to be much smaller than one, resulting in [1], [6]

$$f_{\mathbf{Y}}(\mathbf{y} | M_0) \approx f_{\mathbf{Y}}(\mathbf{y} | \mathbf{0}). \quad (2)$$

Using (2) and assuming that the transform coefficients are statistically independent, we can express the likelihood ratio as

$$\begin{aligned} l(\mathbf{y}) &= \frac{\prod_{i=1}^N f_{Y_i}(y_i | w_i^*)}{\prod_{i=1}^N f_{Y_i}(y_i | 0)} \\ &= \prod_{i=1}^N \frac{\frac{1}{1+\alpha_i w_i^*} f_{X_i}\left(\frac{y_i}{1+\alpha_i w_i^*}\right)}{\prod_{i=1}^N f_{X_i}(y_i)}. \end{aligned} \quad (3)$$

Taking the natural logarithm of the likelihood ratio, the decision rule becomes

$$z(\mathbf{y}) = \sum_{i=1}^N \left[\ln f_{X_i} \left(\frac{y_i}{1 + \alpha_i w_i^*} \right) - \ln f_{X_i}(y_i) \right] > \lambda' \quad (4)$$

where $\lambda' = \ln \lambda + \sum_{i=1}^N \ln(1 + \alpha_i w_i^*)$ is the modified decision threshold.

IV. DECISION THRESHOLD

The Neyman–Pearson criterion can be used to obtain λ' in such a way that the missed detection probability is minimized, subject to a fixed false alarm probability, say, P_{FA}^* . In view of (2), it follows that

$$\begin{aligned} P_{FA}^* &= P(z(\mathbf{Y}) > \lambda' | M_0) = P(z(\mathbf{X}) > \lambda') \\ &= \int_{\lambda'}^{\infty} f_z(\mathbf{x})(z(\mathbf{x})) dz(\mathbf{x}) \end{aligned} \quad (5)$$

where

$$z(\mathbf{x}) = z(\mathbf{y})|_{\mathbf{y}=\mathbf{x}} = \sum_{i=1}^N \left[\ln f_{X_i} \left(\frac{x_i}{1 + \alpha_i w_i^*} \right) - \ln f_{X_i}(x_i) \right]$$

is the realization of the random variable $z(\mathbf{X})$. By the central limit theorem, the PDF of $z(\mathbf{X})$ can be assumed to be Gaussian with mean

$$\begin{aligned} \mu_z(\mathbf{X}) &= E[z(\mathbf{X})] \\ &= \sum_{i=1}^N E \left[\ln f_{X_i} \left(\frac{x_i}{1 + \alpha_i w_i^*} \right) - \ln f_{X_i}(x_i) \right] \end{aligned} \quad (6)$$

and variance

$$\begin{aligned} \sigma_z^2(\mathbf{X}) &= V[z(\mathbf{X})] \\ &= \sum_{i=1}^N V \left[\ln f_{X_i} \left(\frac{x_i}{1 + \alpha_i w_i^*} \right) - \ln f_{X_i}(x_i) \right]. \end{aligned} \quad (7)$$

Thus, we can write (5) as

$$\begin{aligned} P_{FA}^* &= \int_{\lambda'}^{\infty} \frac{1}{\sqrt{2\pi\sigma_z^2(\mathbf{X})}} \exp \left(-\frac{(z(\mathbf{x}) - \mu_z(\mathbf{X}))^2}{2\sigma_z^2(\mathbf{X})} \right) dz(\mathbf{x}) \\ &= \frac{1}{2} \operatorname{erfc} \left(\frac{\lambda' - \mu_z(\mathbf{X})}{\sqrt{2\sigma_z^2(\mathbf{X})}} \right) \end{aligned} \quad (8)$$

where $\operatorname{erfc}(\cdot)$ is the complementary error function, such that

$$\lambda' = \operatorname{erfc}^{-1}(2P_{FA}^*) \sqrt{2\sigma_z^2(\mathbf{X})} + \mu_z(\mathbf{X}). \quad (9)$$

As a rule of thumb, the value of N should be at least 30 for the application of the central limit theorem [3].

V. LAPLACIAN MODEL

The Laplacian PDF is commonly used to model coefficients of discrete cosine transform (DCT) [2]. Here, we consider mod-

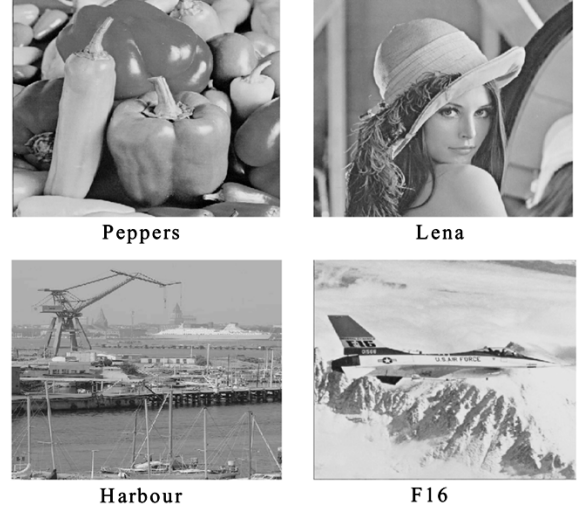


Fig. 1. Test Images.

eling the DWT coefficient X_i by a Laplacian PDF, which is defined as

$$f_{X_i}(x_i) = 0.5b_i \exp(-b_i|x_i - \mu_i|), \quad -\infty < x_i < \infty \quad (10)$$

with $b_i = \sqrt{2}/\sigma_i$, where σ_i^2 is the variance of X_i , and μ_i is the mean of X_i . Substituting (10) in (4), we obtain the decision rule as

$$z(\mathbf{y}) = \sum_{i=1}^N b_i [|y_i - \mu_i| - |1 + \alpha_i w_i^*|^{-1} |y_i - \mu_i - \mu_i \alpha_i w_i^*|] > \lambda'. \quad (11)$$

In Appendix A, it is shown that the mean and variance of $z(\mathbf{X})$ are given as

$$\begin{aligned} \mu_z(\mathbf{X}) &= \sum_{i=1}^N [1 - |1 + \alpha_i w_i^*|^{-1} \{b_i |\mu_i \alpha_i w_i^*| \\ &\quad + \exp(-b_i |\mu_i \alpha_i w_i^*|)\}] \end{aligned} \quad (12)$$

and

$$\begin{aligned} \sigma_z^2(\mathbf{X}) &= \sum_{i=1}^N [1 + |1 + \alpha_i w_i^*|^{-2} \{2 - \exp(-2b_i |\mu_i \alpha_i w_i^*|) \\ &\quad - 2|1 + \alpha_i w_i^*|^{-1} \exp(-b_i |\mu_i \alpha_i w_i^*|) \\ &\quad - 2b_i |\mu_i \alpha_i w_i^*| \exp(-b_i |\mu_i \alpha_i w_i^*|) \{ |1 + \alpha_i w_i^*|^{-1} \\ &\quad + |1 + \alpha_i w_i^*|^{-2} \} \}] \end{aligned} \quad (13)$$

respectively. Thus, substituting (12) and (13) in (9), we obtain the decision threshold λ' .

VI. EXPERIMENTAL RESULTS

The Laplacian model is compared with the Gaussian model [5] using 512×512 test images, as shown in Fig. 1. Each image is transformed by DWT using a Daubechies filter to obtain a three-level pyramid decomposition [4]. Watermark embedding is done in the high-resolution subbands LH_3 , HL_3 and HH_3 . Each subband has 4096 identically distributed coefficients, and therefore, $N = 12 \times 288$.

TABLE I
PERCENTAGE OF SUCCESSFUL DETECTIONS UNDER JPEG COMPRESSION

| Image | Laplacian Model | Gaussian Model |
|---------|-----------------|----------------|
| Peppers | 96.23 | 81.95 |
| Lena | 91.41 | 83.61 |
| Harbour | 95.63 | 85.89 |
| F16 | 98.11 | 91.43 |

TABLE II
PERCENTAGE OF SUCCESSFUL DETECTIONS UNDER BLURRING

| Image | Laplacian Model | Gaussian Model |
|---------|-----------------|----------------|
| Peppers | 93.17 | 85.69 |
| Lena | 89.38 | 86.35 |
| Harbour | 92.62 | 90.16 |
| F16 | 97.21 | 84.63 |

TABLE III
PERCENTAGE OF SUCCESSFUL DETECTIONS UNDER GAUSSIAN NOISE

| Image | Laplacian Model | Gaussian Model |
|---------|-----------------|----------------|
| Peppers | 89.26 | 87.46 |
| Lena | 91.45 | 90.67 |
| Harbour | 97.10 | 87.31 |
| F16 | 96.41 | 91.18 |

Blind detection is used, i.e., the original image is not required in the detection process. This is done by estimating the mean μ_i and variance σ_i^2 possibly from the distorted watermarked image. Let B be one of the subbands LH_3 , HL_3 , and HH_3 . If $x_i \in B$, then μ_i and σ_i^2 are estimated from the unbiased estimators $\hat{\mu}_i = (1/N_B) \sum_{y \in B} y$ and $\hat{\sigma}_i^2 = (1/(N_B - 1)) \sum_{y \in B} (y - \hat{\mu}_i)^2$, respectively, where $N_B = 4096$ and y is the corresponding DWT coefficient in B of the watermarked image.

A constant embedding strength α is used for all the coefficients in LH_3 , HL_3 , and HH_3 . The value of α is chosen so that the peak signal-to-noise ratio (PSNR) of each watermarked image is about 45 dB.

With $P_{FA}^* = 10^{-9}$, the robustness of the watermark is tested under different standard image processing operations. Table I shows the results for watermarked images compressed by JPEG with a 50% quality factor. In Table II, the watermarked images are blurred using a 4×4 spatial filter, and in Table III, they are corrupted by Gaussian noise of zero mean and variance equal to 0.5. These results are based on 10 000 trials. In each trial, we embed into each image a watermark \mathbf{w}^* chosen from a set W of 100 randomly generated watermarks. A detection is said to be successful only if the decision threshold is exceeded for the watermark \mathbf{w}^* but not for any other watermarks in W . Our simulation results reveal that the Laplacian model generally yields a better watermark detection than the Gaussian model.

VII. CONCLUSION

An ML detection scheme based on modeling the distribution of the image DWT coefficients using a Laplacian PDF is formulated. By use of the Neyman–Pearson criterion, a decision threshold is explicitly derived. The Laplacian model is compared with the Gaussian model. Our set of experiments reveal

that the Laplacian model results in a better detection performance. Further research will focus on giving a more comprehensive performance evaluation of these models that includes robustness under other standard image processing operations.

APPENDIX A

In view of (11), to prove (12) and (13), we need to obtain the mean and variance of

$$\phi_i(X_i) = b_i[|X_i - \mu_i| - |1 + \alpha_i w_i^*|^{-1}|X_i - \mu_i - \mu_i \alpha_i w_i^*|].$$

First, we derive the mean of $\phi_i(X_i)$. It is straightforward to show that

$$E[|X_i - \mu_i|] = b_i^{-1}. \quad (14)$$

If $\mu_i \alpha_i w_i^* > 0$, then

$$\begin{aligned} E[|X_i - \mu_i - \mu_i \alpha_i w_i^*|] &= 0.5 b_i \left\{ \int_{-\infty}^{\mu_i} -(x_i - \mu_i - \mu_i \alpha_i w_i^*) \right. \\ &\quad \times \exp(b_i(x_i - \mu_i)) dx_i \\ &\quad + \int_{\mu_i}^{\mu_i + \mu_i \alpha_i w_i^*} -(x_i - \mu_i - \mu_i \alpha_i w_i^*) \\ &\quad \times \exp(-b_i(x_i - \mu_i)) dx_i \\ &\quad + \int_{\mu_i + \mu_i \alpha_i w_i^*}^{+\infty} (x_i - \mu_i - \mu_i \alpha_i w_i^*) \\ &\quad \times \exp(-b_i(x_i - \mu_i)) dx_i \left. \right\}. \end{aligned} \quad (15)$$

By evaluating each integral using integration by parts, we obtain

$$E[|X_i - \mu_i - \mu_i \alpha_i w_i^*|] = \mu_i \alpha_i w_i^* + b_i^{-1} \exp(-b_i \mu_i \alpha_i w_i^*). \quad (16)$$

Similarly, if $\mu_i \alpha_i w_i^* < 0$, then

$$E[|X_i - \mu_i - \mu_i \alpha_i w_i^*|] = -\mu_i \alpha_i w_i^* + b_i^{-1} \exp(b_i \mu_i \alpha_i w_i^*). \quad (17)$$

Combining (16) and (17) yields

$$\begin{aligned} E[|X_i - \mu_i - \mu_i \alpha_i w_i^*|] &= |\mu_i \alpha_i w_i^*| + b_i^{-1} \exp(-b_i |\mu_i \alpha_i w_i^*|). \end{aligned} \quad (18)$$

Thus, using (14) and (18), we obtain the mean of $\phi_i(X_i)$ and, hence, the mean of $z(\mathbf{X})$, as given in (12).

Having found the mean of $\phi_i(X_i)$, we need to derive $E[\phi_i^2(X_i)]$. We can express $E[\phi_i^2(X_i)]$ as

$$\begin{aligned} E[\phi_i^2(X_i)] &= b_i^2 \{ E[|X_i - \mu_i|^2] + |1 + \alpha_i w_i^*|^{-2} \\ &\quad \times E[|X_i - \mu_i - \mu_i \alpha_i w_i^*|^2] - 2|1 + \alpha_i w_i^*|^{-1} \\ &\quad \times E[|X_i - \mu_i||X_i - \mu_i - \mu_i \alpha_i w_i^*|] \}. \end{aligned} \quad (19)$$

Note that

$$E[|X_i - \mu_i|^2] = \sigma_i^2 = 2b_i^{-2} \quad (20)$$

and

$$E[|X_i - \mu_i - \mu_i \alpha_i w_i^*|^2] = 2b_i^{-2} + (\mu_i \alpha_i w_i^*)^2. \quad (21)$$

Following the same approach used to derive (18), it can be shown that

$$\begin{aligned} E[|X_i - \mu_i||X_i - \mu_i - \mu_i \alpha_i w_i^*|] \\ = b_i^{-1} |\mu_i \alpha_i w_i^*| (1 + \exp(-b_i |\mu_i \alpha_i w_i^*|)) \\ + 2b_i^{-2} \exp(-b_i |\mu_i \alpha_i w_i^*|). \end{aligned} \quad (22)$$

Combining these terms yields $E[\phi_i^2(X_i)]$, and together with $E^2[\phi_i(X_i)]$, the variance of $z(\mathbf{X})$ can be expressed, as shown in (13).

REFERENCES

- [1] M. Barni, F. Bartolini, A. De Rosa, and A. Piva, "A new decoder for the optimum recovery of nonadditive watermarks," *IEEE Trans. Image Process.*, vol. 10, no. 5, pp. 755–766, May 2001.
- [2] Q. Cheng and T. S. Huang, "A DCT-domain blind watermarking system using optimum detection on Laplacian model," in *Proc. Int. Conf. Image Process.*, vol. 1, Vancouver, BC, Canada, 2000, pp. 454–457.
- [3] J. L. Devore, *Probability and Statistics for Engineering and the Sciences*. Pacific Grove, CA: Brooks/Cole, 2004.
- [4] Y.-S. Kim, O.-H. Kwon, and R.-H. Park, "Wavelet based watermarking method for digital images using the human visual system," *Electron. Lett.*, vol. 35, no. 6, pp. 466–468, Mar. 1999.
- [5] S.-G. Kwon, S.-H. Lee, K.-K. Kwon, K.-R. Kwon, and K.-I. Lee, "Watermark detection algorithm using statistical decision theory," in *Proc. IEEE Int. Conf. Multimedia Expo.*, vol. 1, 2002, pp. 561–564.
- [6] T. M. Ng and H. K. Garg, "Wavelet domain watermarking using maximum-likelihood detection," in *Proc. SPIE Conf. Security, Steganography, Watermarking Multimedia Contents VI*, vol. 5306, San Jose, CA, 2004.